D.V. Efremov Scientific Research Institute
of Electrophysical Apparatus

Scientific Technical Center SINTEZ

Scientific Technical Center TEMP

A Technical Proposal for the Development and Manufacturing of Electromagnets for the TESLA Beam Delivery System

E.Bondarchuk, N.Doinikov, V.Muratov, V.Peregud, A.Popov

TESLA 2000-23
18 October, 2000

I. Introduction

Under Attachment #019 to the Agreement between Deutsches Elektronensychroton and the D.V. Efremov Scientific Research Institute of Electrophysical Apparatus dated April 29, 1997 the Efremov Institute performed the works on defining the most important parameters and the manufacturing cost of the batch of electromagnets of different types intended for the electron beam transportation system for the TESLA linear accelerator rated for 400 GeV energy.

The basis for the work to be performed was the scheme of the electron beam channel provided by DESY in the form of a table (see Appendix 1, Table I.1 «TESLA BDS vs. 8 magnets» dated 24 February 2000) with the list of beam bending and focusing magnets with their main parameters: the length, L, the aperture radius, R_p, the pole tip field, B_p, multipole components, b_n, the size of the «good field» region, GFR. The Table enlisted the quadrupole magnets with an aperture radius of 6.2 mm, a length from 1 m to 2 m and an induction level from 0.008 to 1.266 T; the sextupole magnets with an aperture radius of 6.2 mm, a length from 0.5 to 1 m and an induction from 0.047 to 0.513 T; the dipole bending magnets with a gap of 12.4 mm, a length from 2.5 to 9 m and an induction level in the gap from 0.014 to 0.511 T; the quadrupole magnets with an aperture radius of 10 mm, a length from 0.5 m to 1 m, an induction of 0.83 T; the sextupole magnets with an aperture radius of 10 mm, a length of 2 m and an indication level from 0.224 to 1.373 T; the dipole bending magnets with a gap of 20 mm, a length of 21.7 m and an induction of 0.047 T; the quadrupole magnets with an aperture radius of 55 mm, a length from 0.5 m to 1.5 m and an induction from 0.079 to 0.967 T. All in all there are 129 magnets of 15 types.

DESY also provided the parameters of the power supplies to be taken into account when developing the magnets:

Type 1	100 A - 400 A	100 V - 150 V
Type 2	50 A -100 A	50 V - 100 V
Type 3	500 A -1000 A	200 V - 500 V
Type 4	10 A - 20 A	20 V - 100 V

The progress of the work was reflected in the table dated 3 March 2000 (see Appendix I, Table I.2). It was decided to exclude from consideration the electromagnets with an aperture radius of 6.2 mm and replace them by electromagnets with an aperture radius of 10 mm, as well as to divide the dipoles with a length of 5 m, 9 m and 21.7 m into several magnets with a length no more than 2-2.5 m to facilitate their manufacturing, transportation, installation, as well as to provide arrangement of vacuum pumps for the chamber every 4-5 m. The length L of the quadrupoles and sextupoles varied in order to reduce modifications and to provide the field on the pole B_p not exceeding B_{max}=1.15-1.2 T. In this case the condition $B_p \cdot L$=const was fulfilled. Finally, the maximum length of the dipole module was accepted equal to L_{max}=2.5 m. As a result the list of magnets for the Project was made up (Appendix I, Table I.3). The total number of different magnets is 326, including 82 dipoles, 101 quadrupoles, 120 magnets with combined functions, 22 sextupoles, 1 octupole.

Certain problems arose when developing the magnets with combined functions (BARC type, see Table I.1). The ratio of the dipole and quadrupole field components in these magnets is such that in the total field its gradient component prevails. On the aperture edge $|b_o| \approx 1/3\,|b_1|$. In this connection a quadrupole with an additional dipole winding was considered. In this case, with hyperbolic poles present, in addition to the dipole component there also emerge field disturbances characterized by the harmonics a_3, a_5, etc. The calculation shows that $(a_3/a_1)_{r=Rp}=\pi/4$, $(a_5/a_1)_{r=Rp}=\pi/96$ (see Appendix II). As follows from these estimates, the sextupole component far exceeds the allowable values ($\sim 10^{-4}$ - 10^{-3}) (see the requirements for the sextupole component, Table I.4). As result of further discussions the like magnets were excluded from the consideration.

On the basis of the above changes Table I.5 dated 19 April 2000 was compiled and the scheme was worked out for arrangement of the magnets along the beam, as shown in Fig.1 (see Appendix I, Table I.6, Fig.1). The problems of the BDS magnet development were discussed in the workshop held at DESY on 4 May, 2000, where it was agreed to replace all electromagnets with 6.2 mm aperture radius by electromagnets with 10 mm aperture radius, the necessity was confirmed to provide additional space of no less than 100 mm for winding overhangs and for installation of vacuum pumps and space of no less than 100 mm for the connecting flanges of the vacuum chamber. In developing each quadrupole it is necessary to take into account that the distance between the quadrupole center and the nearest turns of the coil should be no less than 50-60 mm for installation of the diagnostic apparatus.
Further discussions of the magnet parameters resulted in the elaboration of the Table «TESLA BDS vs. 8.03 magnet data» approved by DESY and the layout of magnets along the beam (Appendix I, Table I.7, Fig.2). The version of dividing the dipole magnets into modules 1.8 m in length was agreed upon and the sizes of the intervals between the magnets necessary to arrange the winding overhangs, the connecting chamber flanges and the vacuum pumps were accepted.

II. Magnet system

The magnet system includes 185 dipoles, 88 quadrupoles, 12 sextupoles and 1 octupole. The main parameters are summarized in Table II.1. The outline drawings for all types of magnets are presented in Attachment II.
All magnets are conventional resistive DC-magnets. The core of most magnets is made as steel lamination 1.5 mm thick. The steel magnetization curve is shown in Fig.II.1. The magnet coils are made from 7.5 mm square copper conductor with a 4.5-mm-diam water-cooled channel. The copper conductor resistivity is no more than 17.2 $m\Omega/mm^2/m$. The coils are water cooled. A pressure drop up to 4 bar is allowed in each of the parallel cooling loop. The coil insulation will be made with vacuum impregnation. The magnetic field in the aperture of the dipoles and quadrupoles varies in a wide range. However, to simplify the design and construction and to reduce the tooling cost the magnets of each type have the same cross-section and are designed for the maximum field. The rest magnets of each type will operate at lower fields.

II.1 Dipoles

All dipoles have 1.8-m-long cores and produce the uniform magnetic field in a 20 mm gap. Flat poles are used to facilitate the manufacturing. All magnets, except septum dipoles, are laminated core magnets of H-type (Fig.II.2). Septum dipoles are solid steel core magnets of H-type, as shown in Fig.II.3. As alternatives considered were also dipoles of C-type with a solid steel core: either with a joint in the middle plane (Fig.II.4) or with demountable poles (Fig.II.5), as well as solid dipoles of H-type (Fig. II.6).
The configuration of the C-type iron core facilitates the vacuum chamber installation and maintenance, as well as simplifies magnetic measurements. It makes no sense to manufacture the C-type dipoles as laminated (Fig.II.7), because it is difficult to provide the geometrical tolerances after stamping and welding.
The final decision on selecting the type of dipole iron core will be made at further design stages.
Each pole has two coil pancakes. Each pancake with 16 turns in 2 layers is made of a square conductor with a water-cooled channel. Each pancake of the C-type magnets can be mounted on the iron core by slipping it through the gap, thus simplifying replacement of a damaged coil. The dipoles operate at different field strength values, as shown in Table II.1. The maximum field for BCDC dipoles is 0.4733 T provided by a current of 242 A at 14 V, this corresponding to a

current density of 6 A/mm^2. Most of the dipoles operate at current densities less than 1.7 A/mm^2. The main parameters of the dipoles are presented in Table II.2.

II.2 Quadrupoles

Table II.3 shows the main parameters of the quadrupoles. Four types of the quadrupole magnets are proposed:

Type A - The majority of the quadrupoles has ∅20 mm aperture. The quadrupoles have the cores of four different lengths: 0.5 m, 1.0 m, 1.5 m and 2 m in length. All quadrupoles have the same in cross-section, as shown in Fig.II.8. Each pole has 26 turns of a square copper conductor. The maximum pole tip field is 1.142 T, requiring 210 A at 34 V with a current density of about 5.2 A/mm^2. Most quadrupoles operate at lower fields than 1.142 T with a correspondingly lower current density. The two-dimensional analysis was made for the maximum field using the POISSON code. The calculated magnetic induction distribution for the quadrupole half-pole e is shown in Fig.II.9. The excitation curve for the quadrupole is shown in Fig.II.10. The calculations also revealed that the amplitude of the 6th harmonic, a_6, depends strongly on the accuracy of the profile of the pole generatrix. Thus, with the interpole gap varying within the limits: d=4.6-4.605 mm, a change in the value $(a_6/a_2)_{r=0.9Rp}$ amounted to $\sim 6\cdot 10^{-4}$ (a_2 - the amplitude of the main harmonic).

The tolerances for the sextupole component in the quadrupoles are presented in Table I.4. The most stringent requirement in this list is imposed on the QCMES quadrupole - $(a_3/a_2)=2\cdot 10^{-4}$. For other quadrupoles the tolerance is not so close. In view of the linear dependence of a_3/a_2 on the radius r on the aperture edge we find:

$$(a_3/a_2)_{Rp=10mm}=5\cdot 10^{-4}\ (*),$$

Let's correlate this tolerance with the similar value attained on the quadrupoles of the Luminosity Upgrade project, where $(a_3/a_2)_{Rp=50mm}\leq 2\cdot 10^{-4}$ was obtained on the QI quadarupole [2]. Should the same tolerance for the quadrupole geometry be provided in quadrupoles with the decreased aperture radius R_p=1- mm, one might expect

$$(a3/a2)Rp=10mm=.10\text{-}3,$$

this exceeding two-fold the allowable field disturbance (*). It means that the manufacturing accuracy of the TESLA BDS quadrupoles must be at least no worse than that attained in [2]. The possibility should be foreseen, as in [2], to compensate for field disturbances by the pole correcting coils.

Type B - The septum quadrupoles QLPA1 and QLPA2 with ∅20 mm aperture have the 1.5-m-long core. A figure of eight-type quadrupoles was chosen because of the limited space for photon beam lines. Each pole has 12 turns of square copper conductor. Maximum current in the winding is 420 A at a current density of 10.5 A/mm2. The quadrupole cross-section is shown in Fig.II.11. The two-dimensional analysis was made using the POISSON code. The calculation results are presented in Fig.II.12 and Fig.II.13.

Type C - The quadrupoles QFT5 and QFT6 with ∅40 mm aperture and 0.5-m-long core. Each pole has 32 turns. The quadrupole cross-section is shown in Fig.II.14.

Type D - The quadrupoles QFT3 and QFT4 with ∅140 mm aperture and 2 m long core. Each pole has 64 turns of square copper conductor. Maximum current in the winding is 400 A at a current density of ~10 A/mm^2, power loss in the winding amounts to 84 kW. The quadrupole cross-section is shown in Fig.II.15.

II.3 Sextupoles

All sextupoles have ∅20 mm aperture and the same cross-section. The sextupole cross-section is shown in Fig.II.16. The two-dimensional analysis was made for a maximum pole tip field of 1.15 T (2 m long sextupole SFCV) using the POISSON code. The calculated magnetic induction distribution for the sextupole half-pole is shown in Fig.II.17. It is seen that in some cross-sections of the poles the induction is as high as 2.4 T. The calculated excitation curve is shown in Fig.II.10. As is seen, the saturation is strong resulting in considerable additional ampere-turns. An increase in the core length up to 2.2 m with an associated field decrease on the pole to 1.05 T caused consumed power to reduce from 12 kW to 7.1 kW. The main parameters of the sextupoles are presented in Table II.4.

II.4 Octupole

The octupole has an aperture 20 mm in diameter and a core 0.5 m in length. The pole tip field is as high as 0.3 T at 34 A (~3 A/mm^2 current density) The cross-section is shown in Fig.II.18. The main parameters are presented in Table II.5.

III. Conclusion

This work has been performed on the basis of estimate of electromagnetic calculations and preliminary studies of the magnet construction.

Reference

[1] POISSON Group Programs User's Guide, 1975.
[2] N. Bogatov, E. Bondarchuk et al., Normal Conducting QI and QJ Quadrupoles for the ITER Luminosity Upgrade, Proc. EPAC-98, Stockholm, p.1963.

TESLA BDS VS.8.03 MAGNET DATA

Table II.1

DIPOLE

№	Label	Number of magnets	Aperture, mm	Core Length, m	Pole tip fields, T
1.	BLPA	28	∅20	L=1,8	0,12
2.	BLPA*)	20			0,12
3.	BLNA	44			0,109
4.	BLNA*)	4			0,109
5.	BFCHO	40			0,0568
6.	BFCVO	40			0,0568
7.	BCBC	3			0,4733
8.	BCMES1	2			0,24
9.	BCMES2	1			0,041
10.	BCMES3	2			0,2408
11.	BCMES4	1			0,111
Σ(1+11)		185			

QUADRUPOLE

№	Label	Number of magnets	Aperture mm	Core Length,m	Pole tip fields, T
1.	QFC1	2	∅20	L=0,5	0,83
2.	QFC4	2			0,83
Σ(1+2)		4			
3.	QLMC1	1	∅20	L=1	0,284
4.	QLMC2	1			0,465
5.	QLMC3	1			1,01
6.	QLMC4	1			0,696
7.	QCMES1	4			0,9745
8.	QCMES2	4			1,143
9.	QCBC1	8			1,041
10.	QCBC2	8			1,1
11.	QFB1	1			0,382
12.	QFB2	1			0,656
13.	QFB3	1			0,738
14.	QFB4	1			0,51
15.	QFB5	1			1
16.	QFB6	1			1
17.	QFC2	7			0,83
18.	QFC3	7			0,83
Σ(3+18)		48			

№	Label	Number of magnets	Aperture mm	Core Length,m	Pole tip fields, T
19.	QLMA1E	1	∅20	L=1,5	0,6515
20.	QLMA2E	1			1,014
21.	QLMA3E	1			0,419
22.	QLMA4E	1	∅20	L=1,5	0,1061
23.	QLPA1	2			0,787
24.	QLPA2	2			0,608
25.	QLNA1	2			0,72
26.	QLNA2	2			0,537
27.	QLPN2	2			0,982
28.	QCMES4	2			0,89
29.	QCMES5	2			0,92
30.	QCMES6	2			1,142
Σ(19+30)		20			
31.	QLPN1	1	∅20	L=2	0,554
32.	QLPN3	1			0,742
33.	QCMES3	4			0,901
34.	QCBC3	8	∅20	L=2	1,024
Σ(31+34)		14			
35.	QFT6	1	∅40	L=0,5	0,647
36.	QFT5	1			0,724
Σ(35+36)		2			
37.	QFT4**	1	∅140	L=2	0,75
38.	QFT3**	1			
Σ(37+38)		2			
Σ(1+38)		90			

SEXTUPOLE

№	Label	Number of magnets	Aperture mm	Core Length, m	Pole tip fields, T
1.	SC1	1	∅20	L=0,5	0,262
2.	SC2	1			0,189
3.	SCS1	1		L=1	0,334
4.	SCS2	1			0,334
5.	SFCH**	4		L=2,2	0,30
6.	SFCH**	4			1,05
Σ(1+6)		12			

OCTUPOLE

№	Label	Number of magnets	Aperture mm	Length, m	Pole tip fields, T
1.	OC	1	∅20	L=0,5	0,285

Total magnet number – 288

*) Septum magnets H-type
**) As compared with Table I.6 (Appendix I),
as the core length is increased so as to reduce the pole tip field and relevant power losses.

The main parameters for the dipoles

Table II.2

№	Label	Air Gap mm	Core Length m	Number of magnets	Magnetic Fields T	Current A	Voltage drop V	Power Loss kW	Total weight kg	Water Flow Rate l /min	Temperature overheating °C
1.	BLPA	20	1,8	28	0,12	62	3,6	0,224	600	0,68	4,7
2.	BLPA (Septum magnet)			20	0,12	62	3,7	0,230	1150		4,8
3.	BLNA			44	0,109	56	3,2	0,18	600		3,8
4.	BLNA (Septum magnet)			4	0,109	56	3,3	0,185	1150		3,8
5.	BSMES1			2	0,24	124	7,1	0,88	600		18,4
6.	BSMES2			1	0,04	20	1,2	0,024			0,5
7.	BSMES3			2	0,240	124	7,1	0,88			18,4
8.	BSMES4			1	0,111	56	3,2	0,18			3,8
9.	BFCH0			40	0,0568	30	1,7	0,051			1,1
10.	BFCVO			40	0,0568	30	1,7	0,051			1,1
11.	BCBC			3	0,4733	242	14	3,4		1,9	26

The main parameters for the quadrupole magnets

Table II.3

№	Label	Aperture mm	Core Length m	Number of magnets	Pole tip fields T	Current A	Voltage drop V	Power loss kW	Total weight kg	Water flow rate l/min	Temperature overheating °C
1.	QFC1			2	0,83	135	9,45	1,3		1,8	10,5
2.	QFC4	∅20	L=0,5	2	0,83	135	9,45	1,3	375	1,8	10,5
3.	QLMC1			1	0,284	46	5,3	0,244		4	1
4.	QLMC2			1	0,465	73	8,35	0,61		4	2,2
5.	QLMC3			1	1,01	170	18,7	3,2		4	11,5
6.	QLMC4			1	0,696	110	12,6	1,34		4	4,8
7.	QCMES1			4	0,9745	162	18,7	3,03		4	11
8.	QCMES2			4	1,143	210	24,2	4,83		4	17,5
9.	QCBC1			8	1,041	173	20	3,46		4	12,5
10.	QCBC2	∅20	L=1,0	8	1,1	188	21,6	4,05	725	4	14,6
11.	QFB1			1	0,382	62	7,1	0,42		4	1,5
12.	QFB2			1	0,656	104	12	1,25		4	4,5
13.	QFB3			1	0,738	120	13,8	1,65		4	4,5
14.	QFB4			1	0,52	81	9,35	0,76		4	2,7
15.	QFB5			1	1,01	170	18,7	3,2		4	11,5
16.	QFB6			1	1,01	170	18,7	3,2		4	11,5
17.	QFC2			7	0,83	135	15,5	2,1		4	7,5
18.	QFC3			7	0,83	135	15,5	2,1		4	7,5
19.	QLMA1E			1	0,6515	104	17	1,75		3,3	7,6
20.	QLMA2E			1	1,014	170	27,6	4,43	1080	3,3	19,5
21.	QLMA3E			1	0,419	66	10,7	0,710		3,3	3,1
22.	QLMA4E			1	0,1061	19	3,1	0,044		3,3	1

№	Label	Aperture mm	Core Length m	Number of magnets	Pole tip fields T	Current A	Voltage drop V	Power loss kW	Total weight kg	Water flow rate l/min	Temperature overheating °C
23.	QLPA1	∅20	L=1,5	2	0,787	420	32,5	14,7	340	5,4	40
24.	QLPA2			2	0,608	330	24	8		5,4	22
25.	QLNA1			2	0,72	110	17,8	2	1080	3,3	8,7
26.	QLNA2			2	0,537	81	13,1	1,06		3,3	4,6
27.	QLPN2			2	0,982	162	26,4	4,3		3,3	19
28.	QCMES4			2	0,89	146	23,65	3,45		3,3	15
29.	QCMES5			2	0,92	150	24,4	3,65		3,3	16
30.	QCMES6			2	1,142	210	34	6,85		3,3	30
31.	QLPN1	∅20	L=2	1	0,554	85	17	1,45	1430	2,9	7
32.	QLPN3			1	0,742	120	24	2,9		2,9	15
33.	QCMES3			4	0,901	104	20,8	2,17		2,9	11
34.	QCBC3			8	1,024	170	34	5,8		2,9	29
35	QFT6	∅40	L=0,5	1	0,647	165	13,7	2,25	500	1,6	20
36.	QFT5			1	0,724	190	15,7	3		1,6	27
37.	QFT4	∅140	L=2,0	1	0,75	400	210	84	4300	30	40
38.	QFT3			1	0,75	400	210	84		30	40

The main parameters for the sextupoles

Table II.4

	SCS1/SCS2	SC1	SC2	SFCH	SFCV
Aperture, mm	∅20	∅20	∅20	∅20	∅20
Core length, m	1	0,5	0,5	2,2	2,2
Number of magnets	1/1	1	1	4	4
Pole tip fields, T	0,336	0,262	0,189	0,3	1,05
Current, A	34	27	17	31	133
Voltage drop, V	6,4	3	1,9	12,3	53
Power loss, kW	0,22	0,081	0,032	0,38	7,1
Total weight, kg	1200	580	580	2650	2650
Water flow rate, l/min	0,4	0,5	0,5	0,3	3,8
Temperature overheating, °C	8	2,3	1,0	18	27

The main parameters for the octupole

Table II.5

	OC
Aperture, mm	∅20
Core length, m	0,5
Number of magnets	1
Pole tip fields, T	0,3
Current, A	34
Voltage drop, V	2,4
Power loss, kW	0,29
Total weight, kg	300
Water flow rate, L/min	1,2
Temperature overheating, °C	3,5

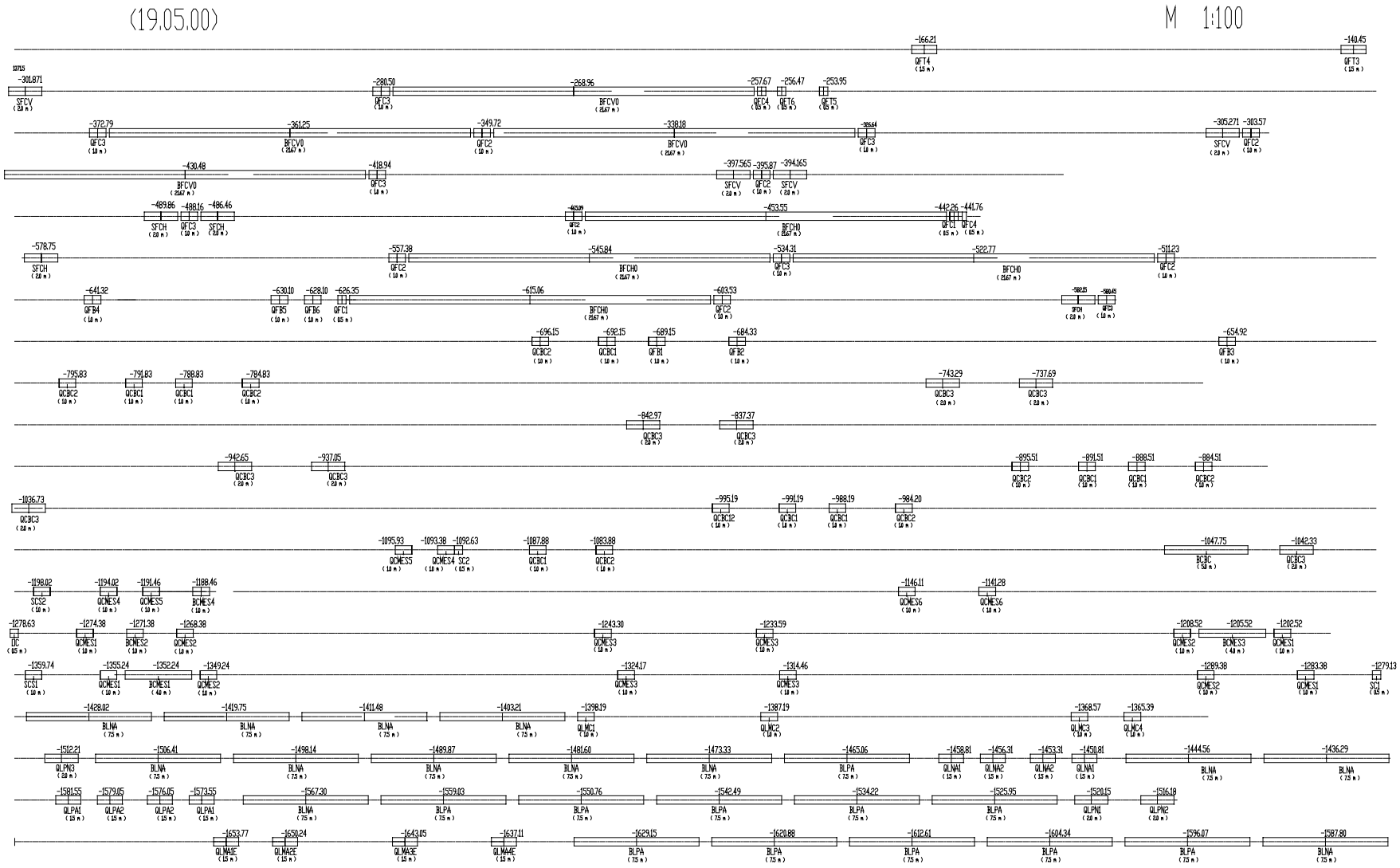

Fig.1 BDS magnets location map along the beam of TESLA accelerator. Vs. 8.02 26.05.2000

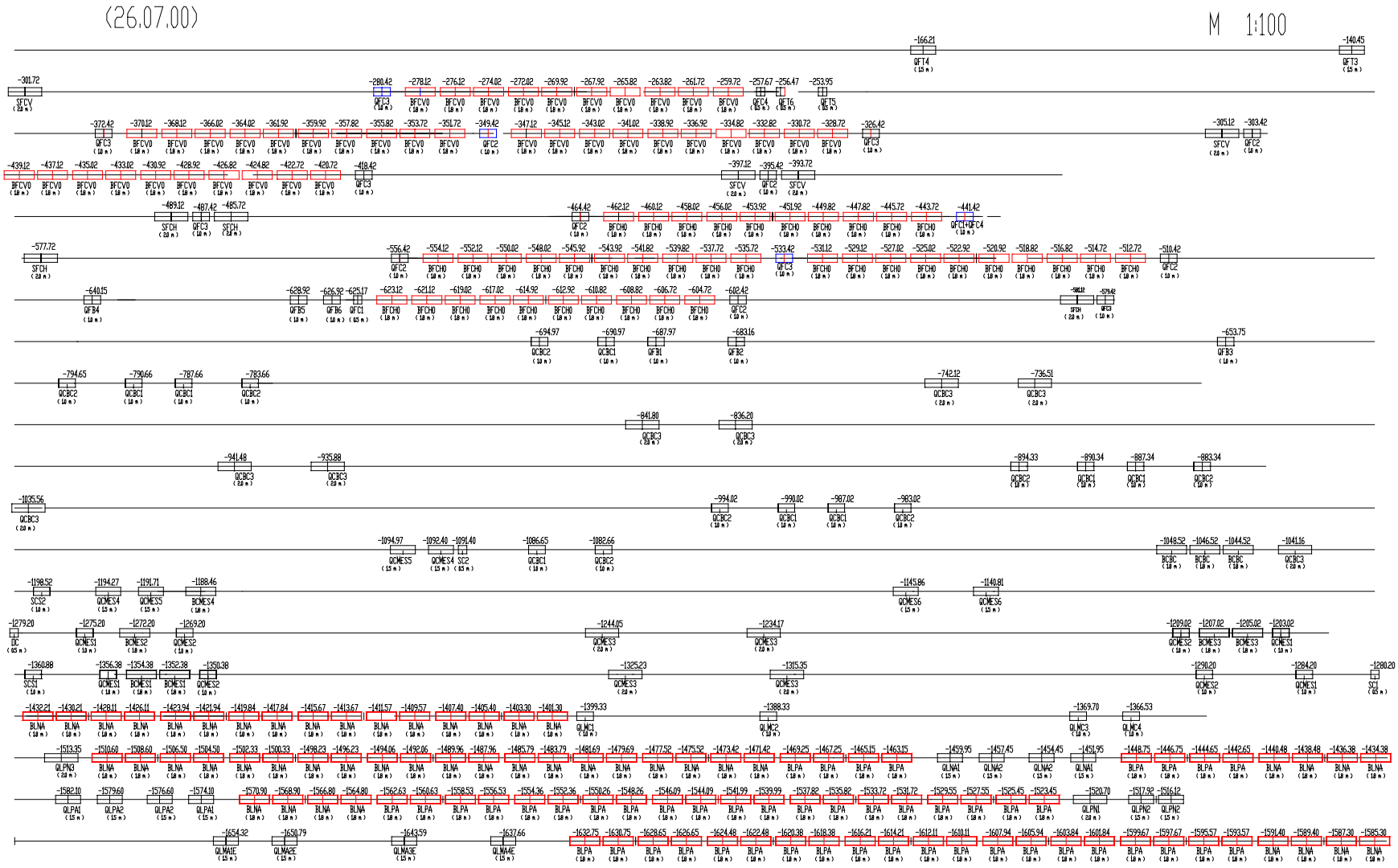

Fig.2 BDS magnets location map along the beam of TESLA accelerator. Vs. 8.03 26.07.2000

Steel 2081

H, [A/M]	B, [T]
0.	0.000
50.	0.028
70.	0.059
100.	0.200
200.	0.764
250.	0.940
350.	1.168
500.	1.339
800.	1.497
1000.	1.542
2500.	1.672
12000.	1.880
20000.	2.000
80000.	2.300

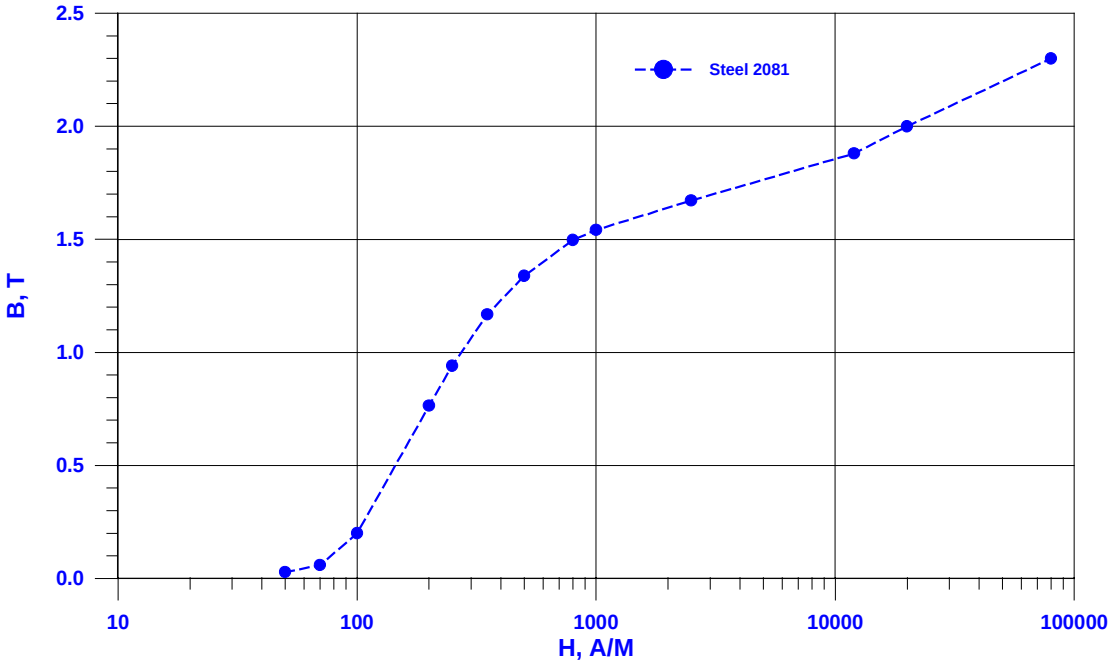

Fig.II.1 The magnetization curve of the magnet steel.

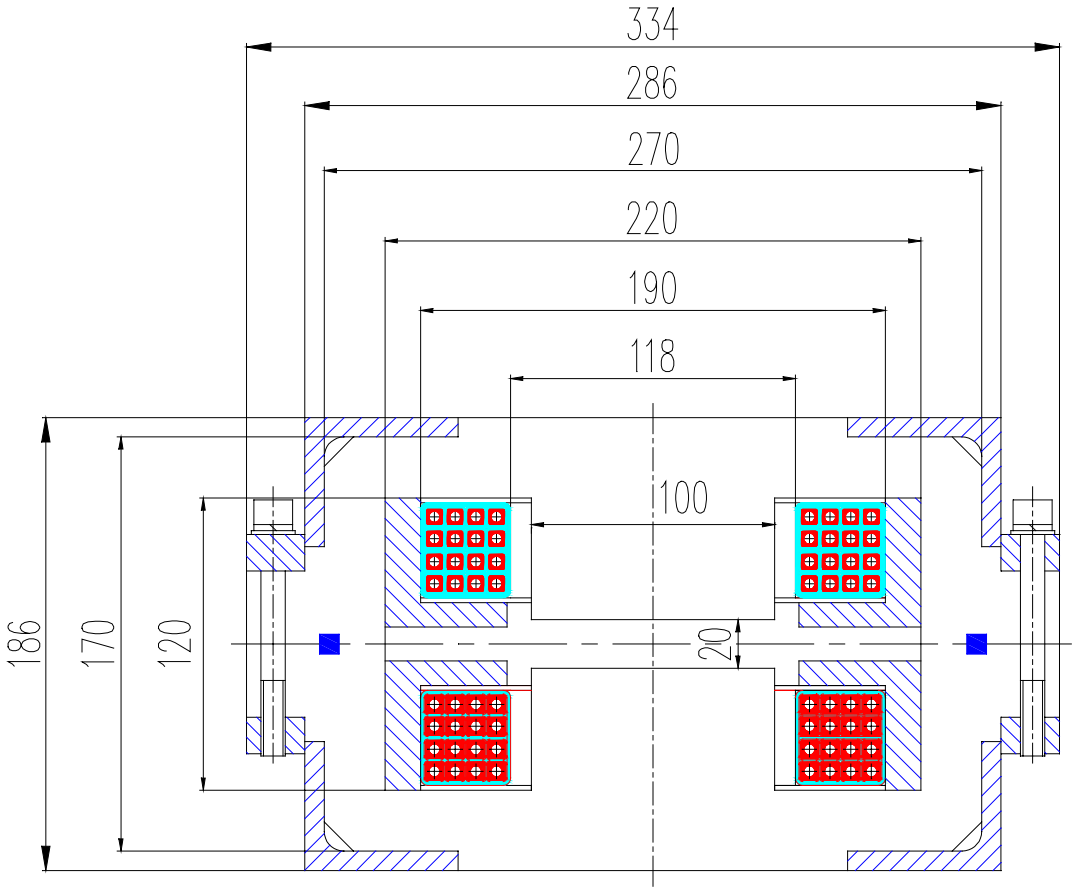

Fig. II.2. The cross section of the dipole H-type (laminated core)

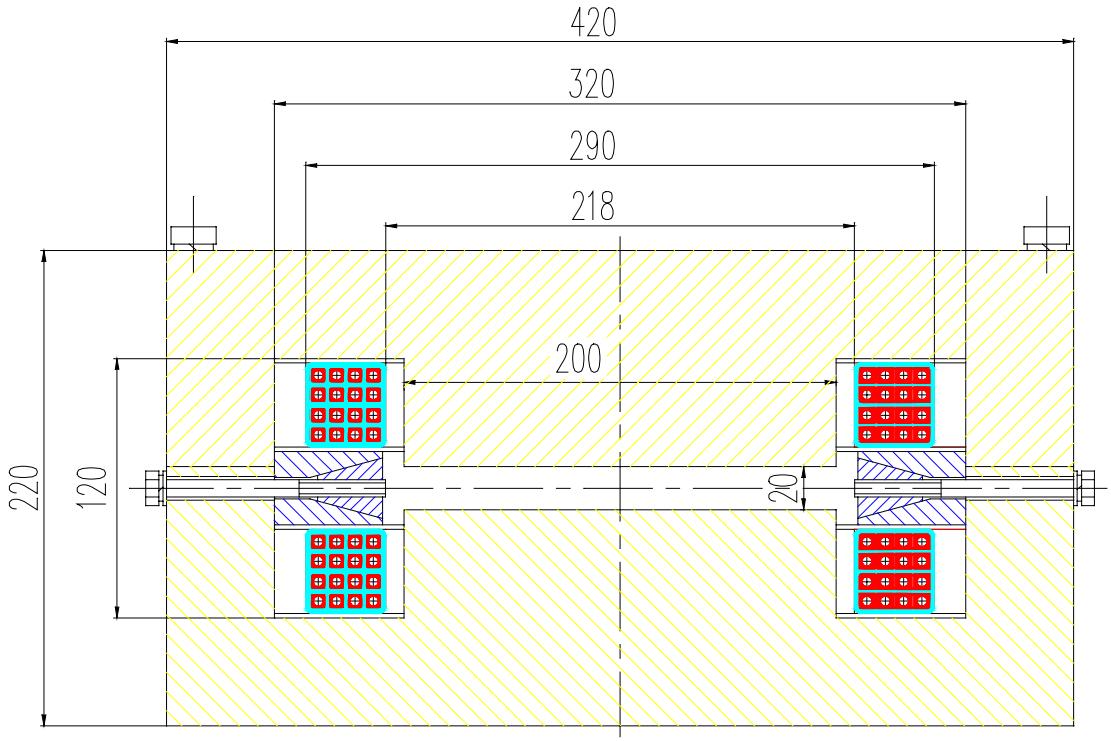

Fig. II.3. The cross-section of the septum dipole (solid steel core)

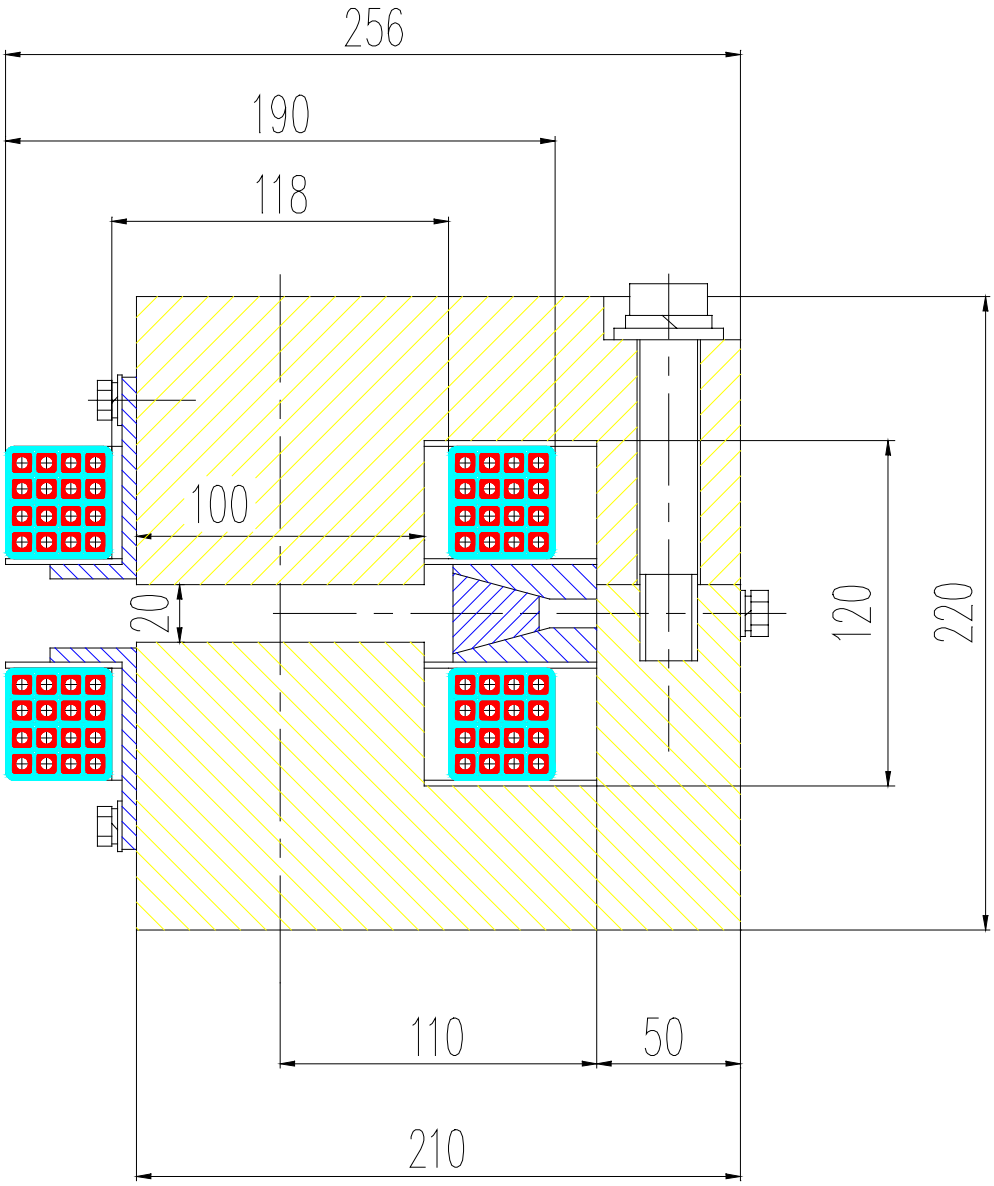

Fig. II.4. The cross section of the dipole C-type (solid steel core)

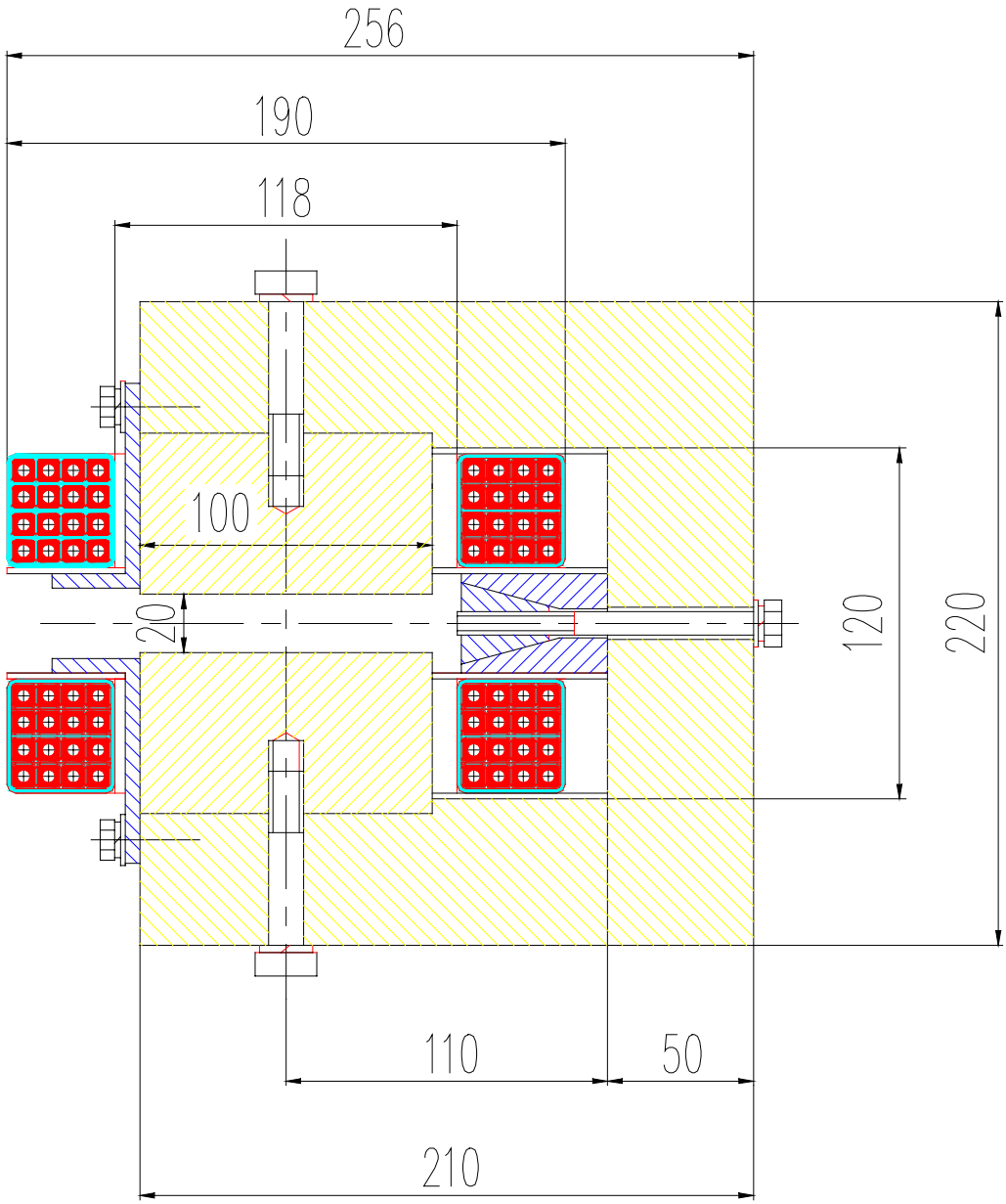

Fig. II.5. The cross section of the dipole C-type (solid steel core)

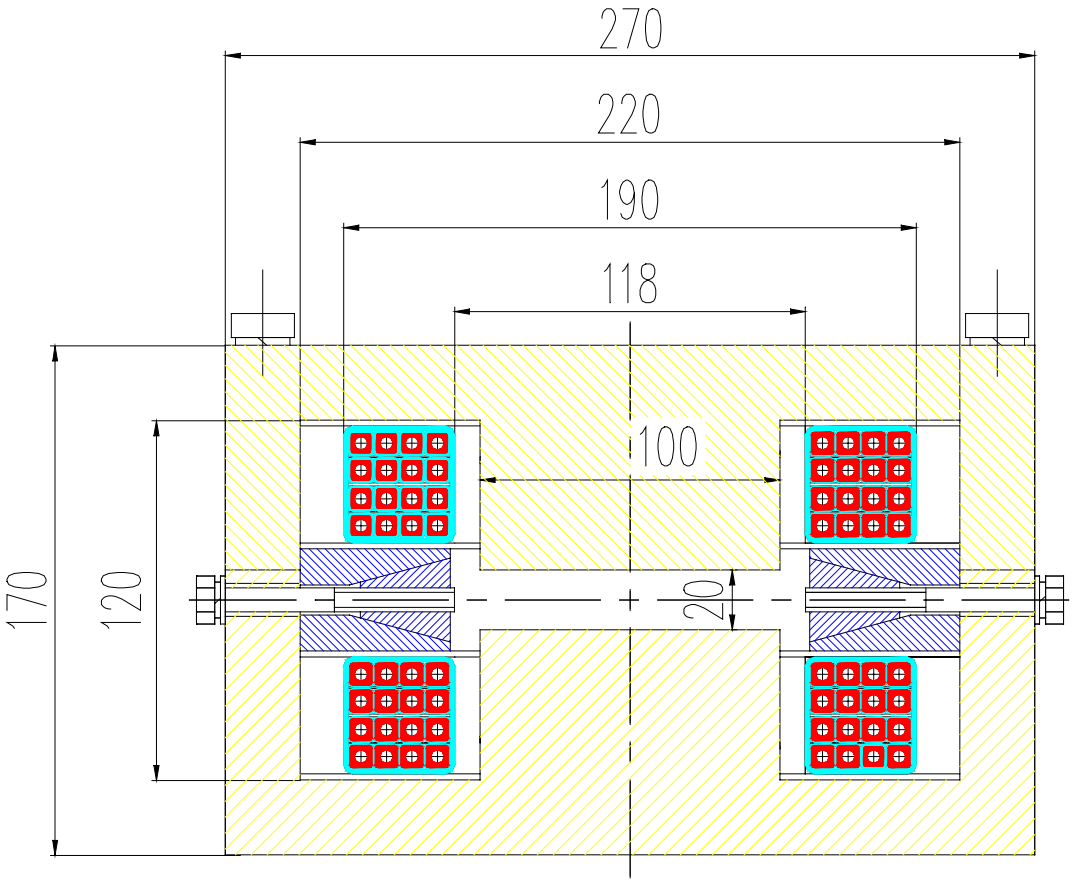

Fig. II.6. The cross section of the dipole H-type (solid steel core)

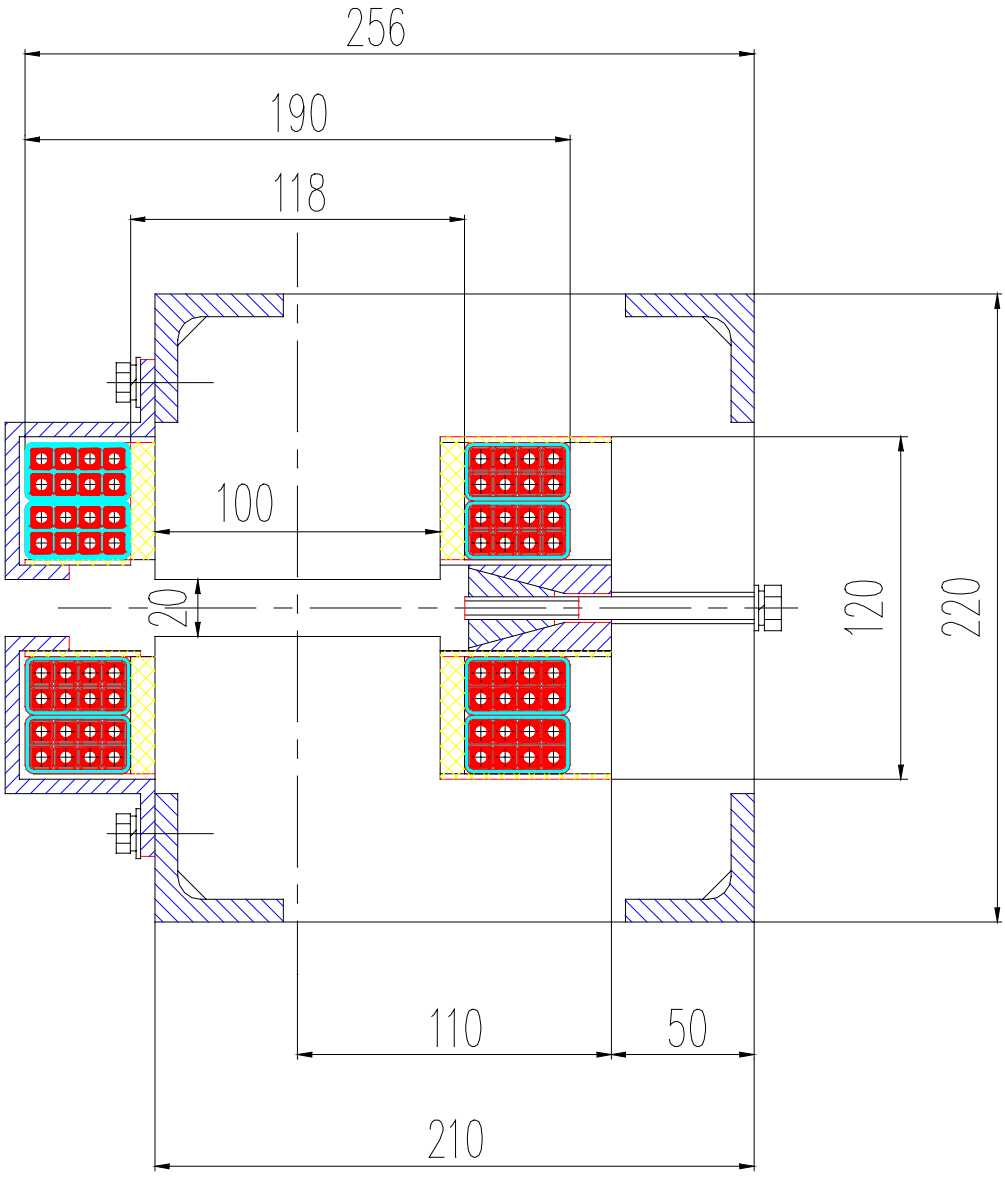

Fig. II.7. The cross section of the dipole C-type (laminated core)

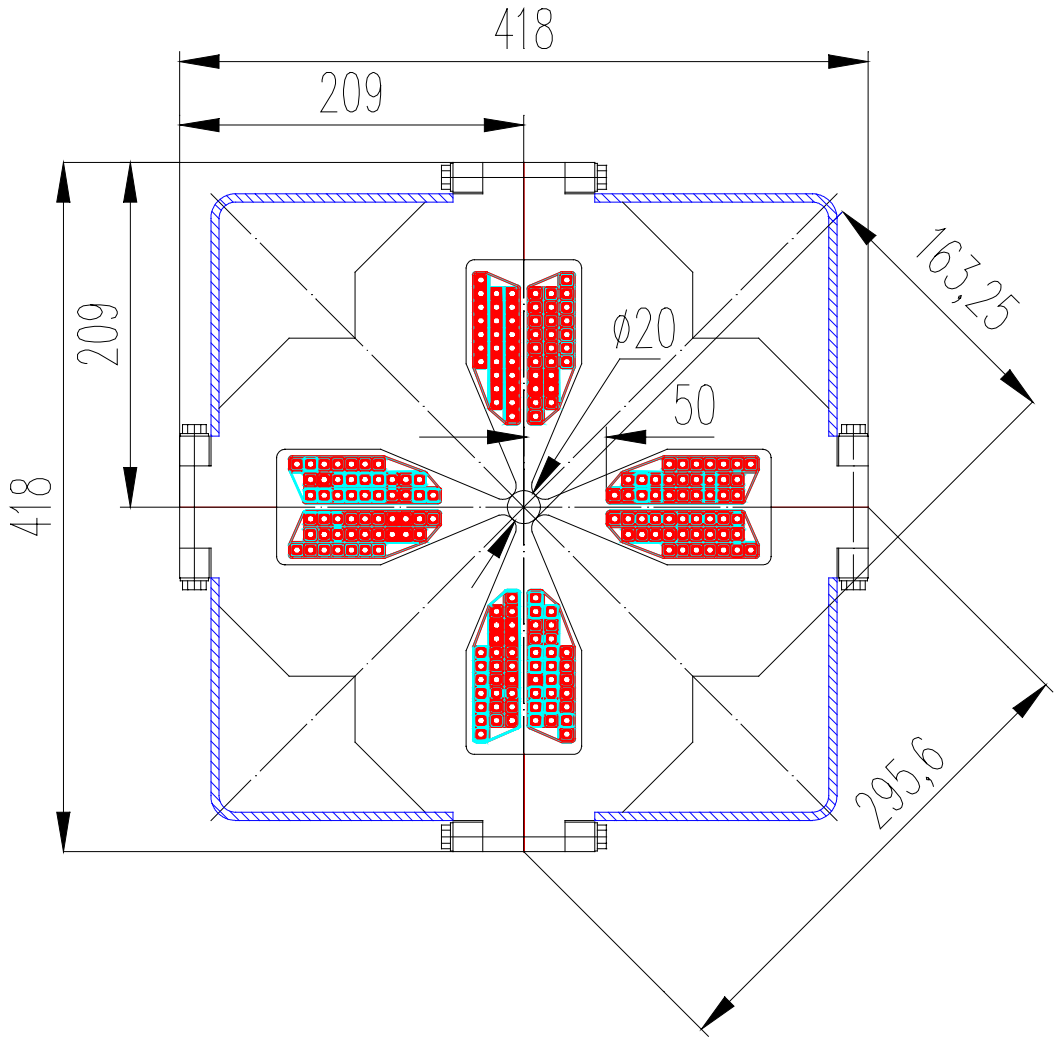

Fig. II.8. The cross section of the quadrupole with the aperture ∅20 mm

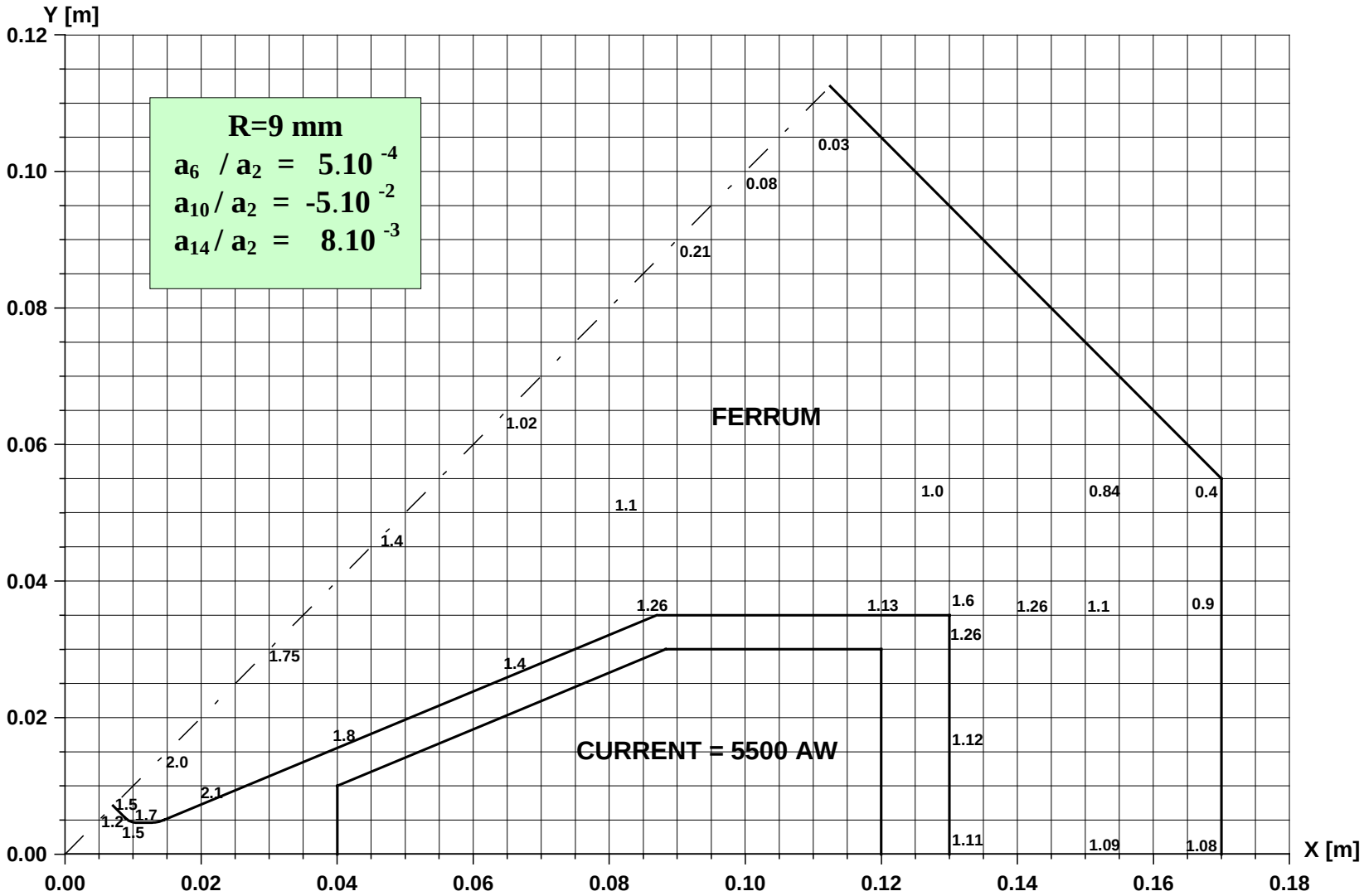

Fig. II.9 The calculated magnetic induction B[T] in some points for half pole of the quadrupole

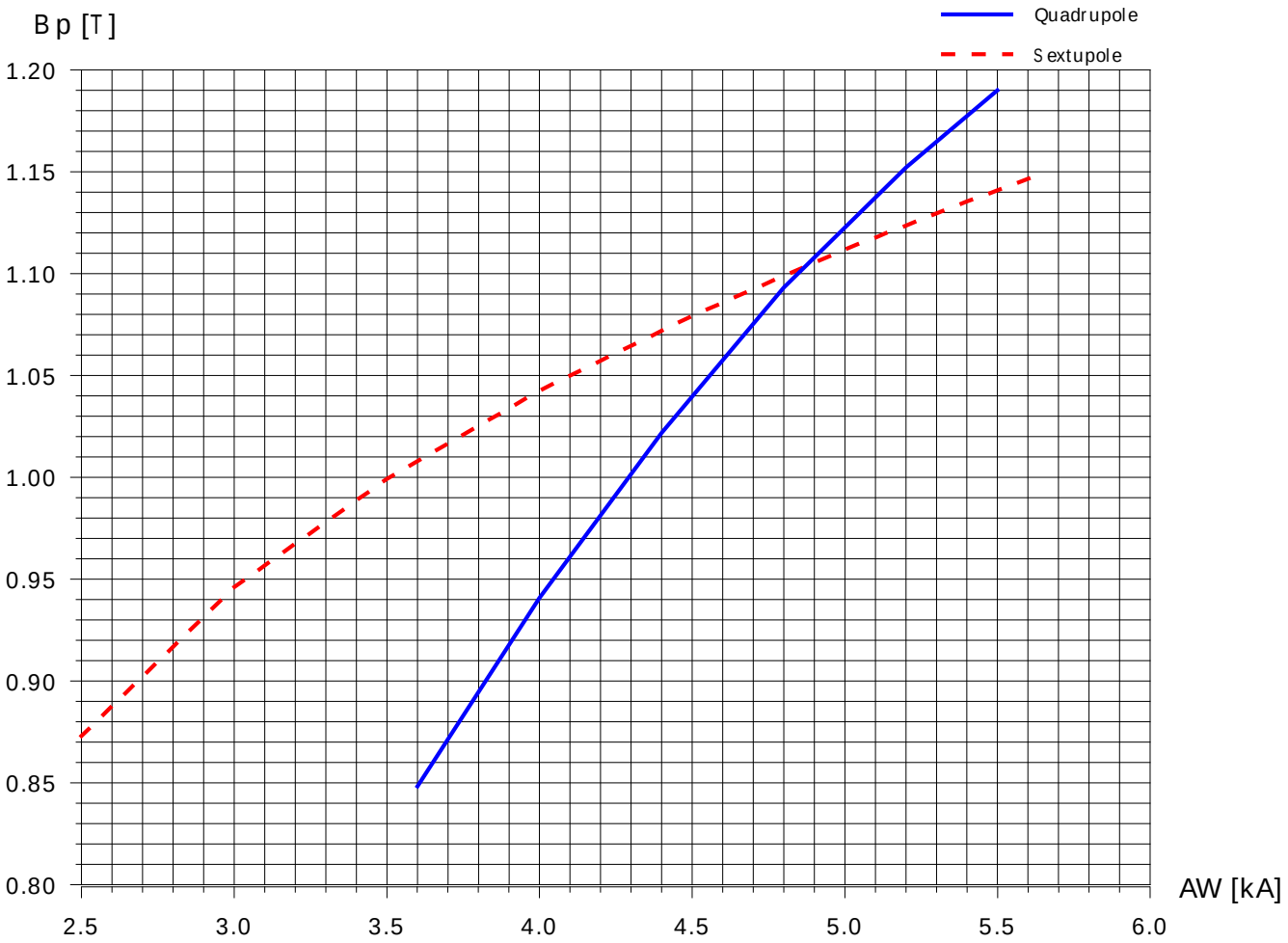

Fig. II.10 The excitation curves of the quadrupole and the sextupole

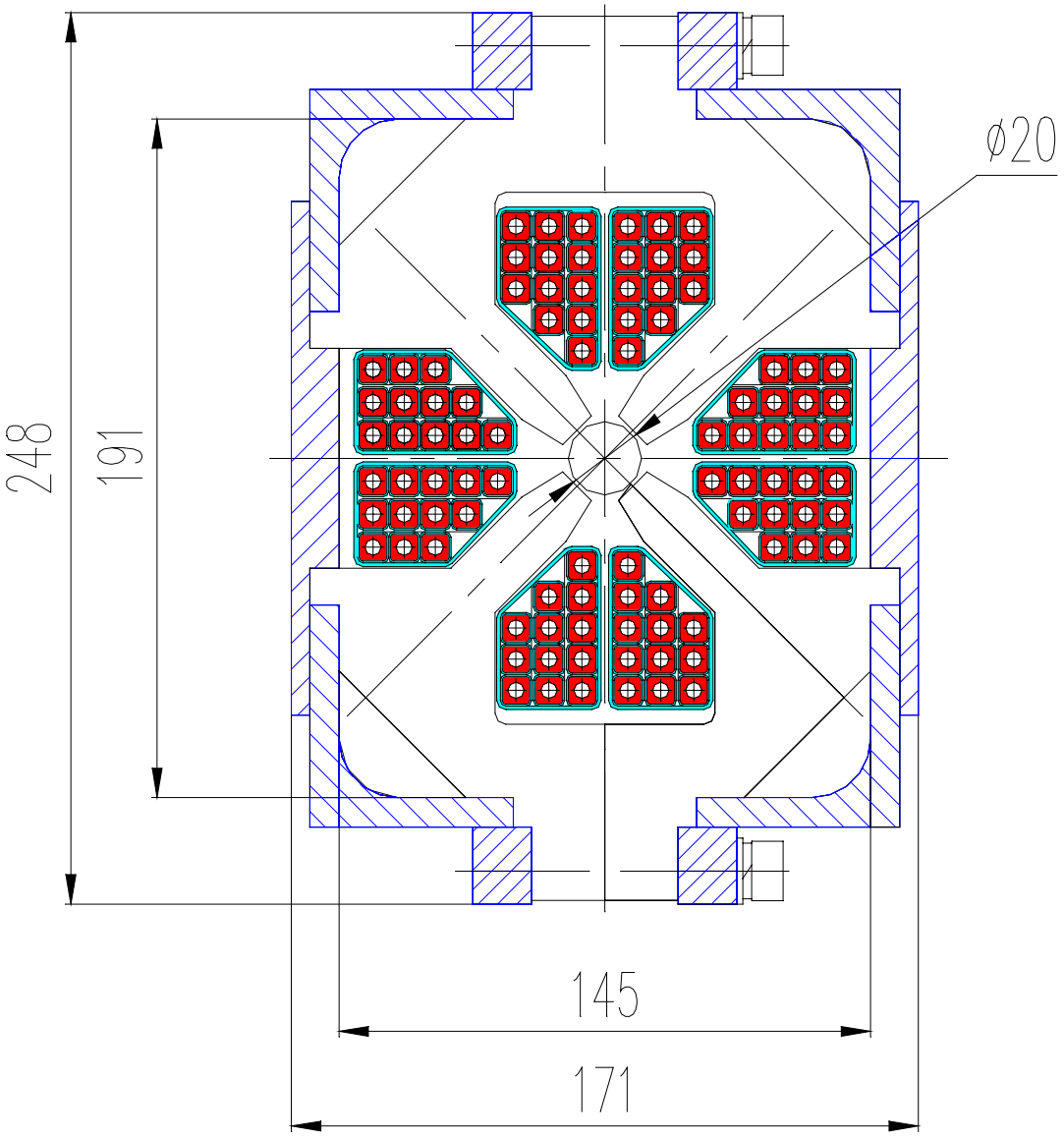

Fig. II.11. The cross section of the septum quadrupole

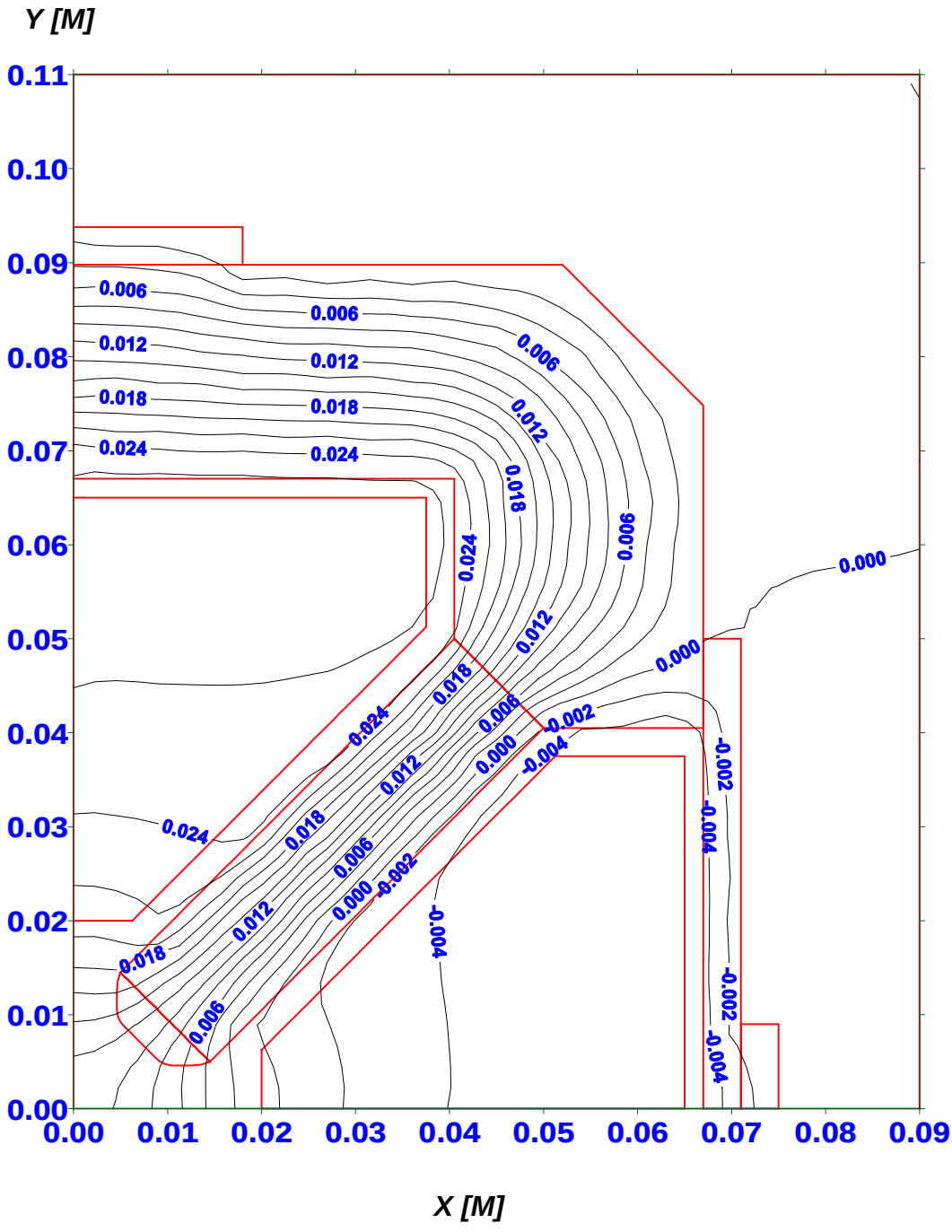

Fig.II.12 The cross section of the septum quadrupole with flux lines.

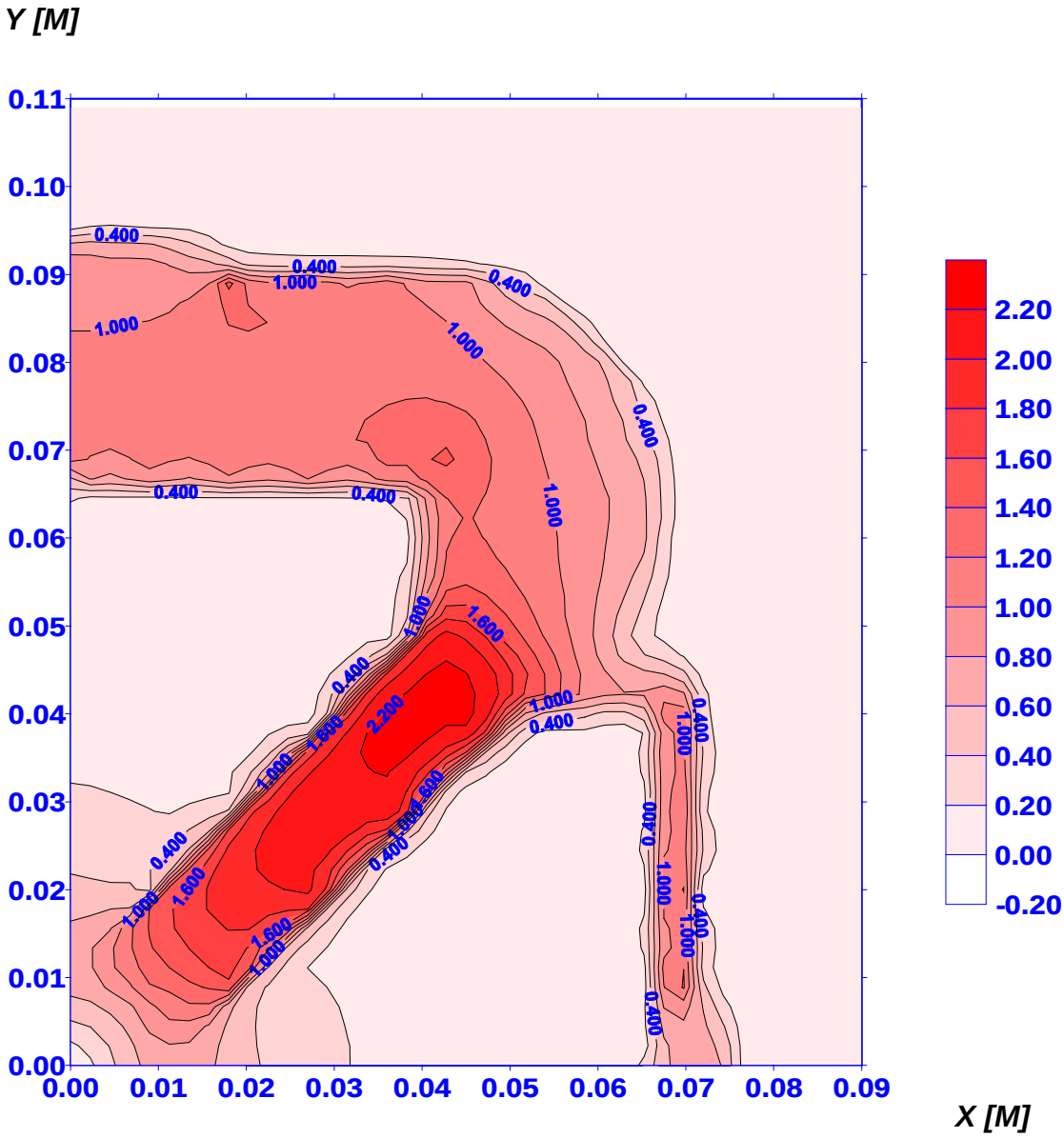

Fig.II.13 The cross section of the septum quadrupole with flux lines.

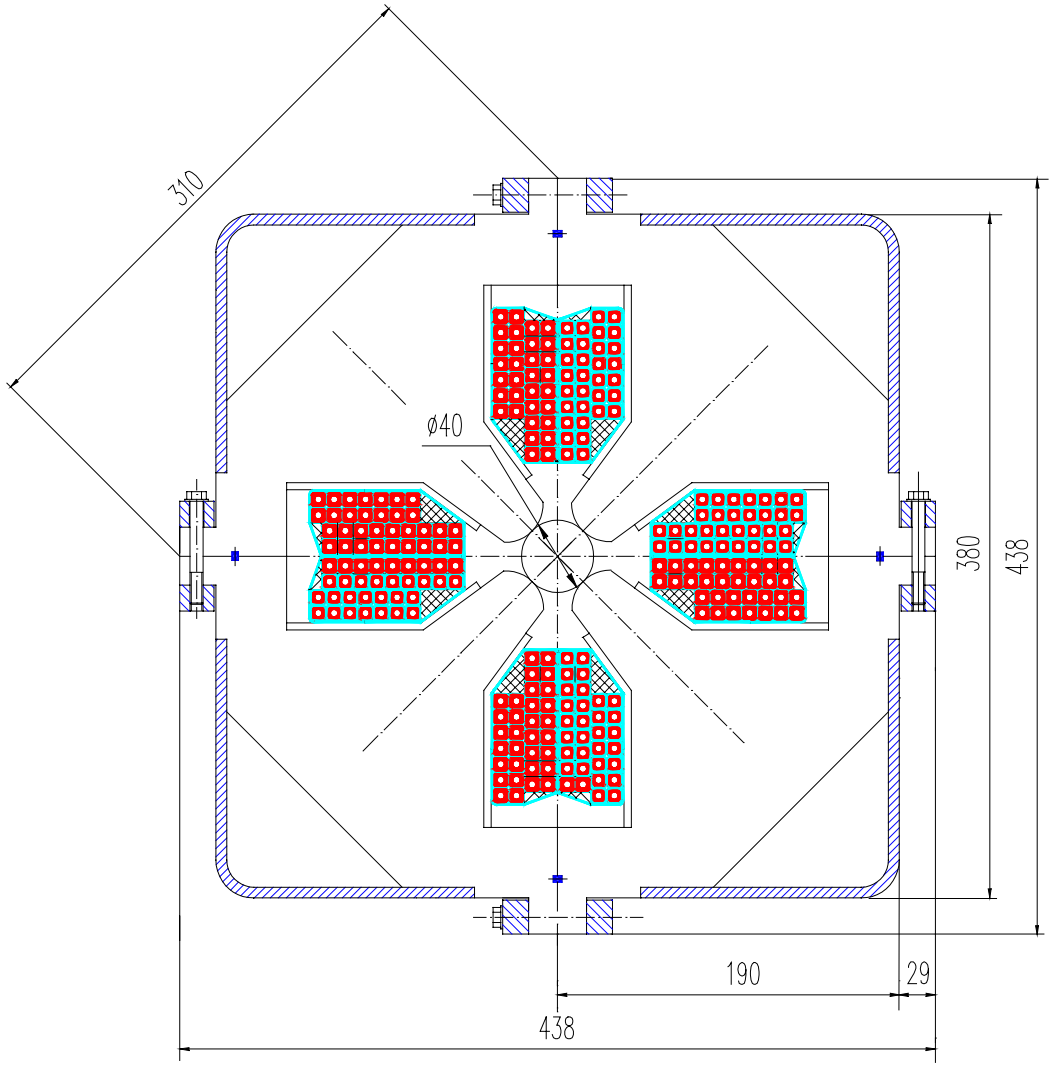

Fig. II.14. The cross section of the quadrupole with the aperture ∅40 mm

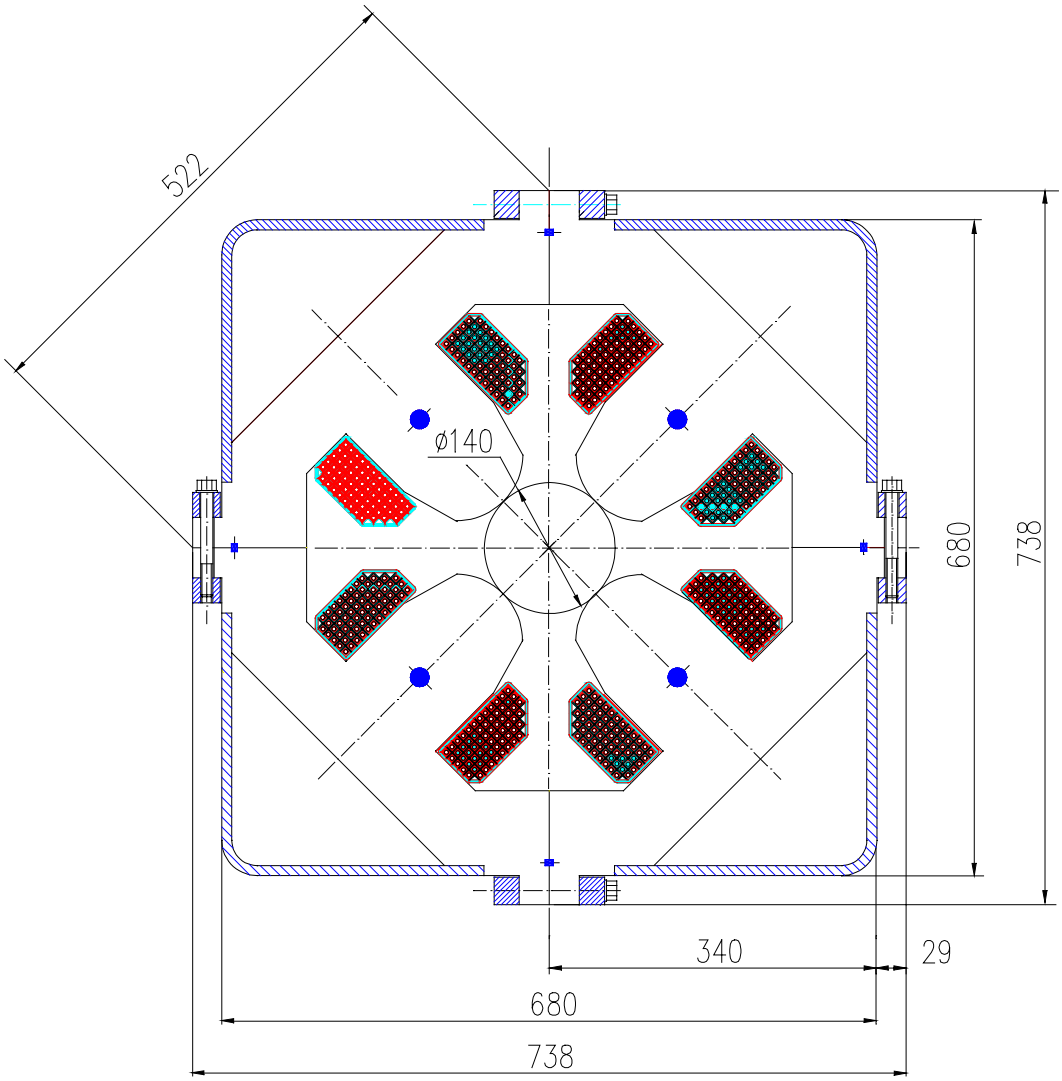

Fig. II.15. The cross section of the quadrupole with the aperture ∅140 mm

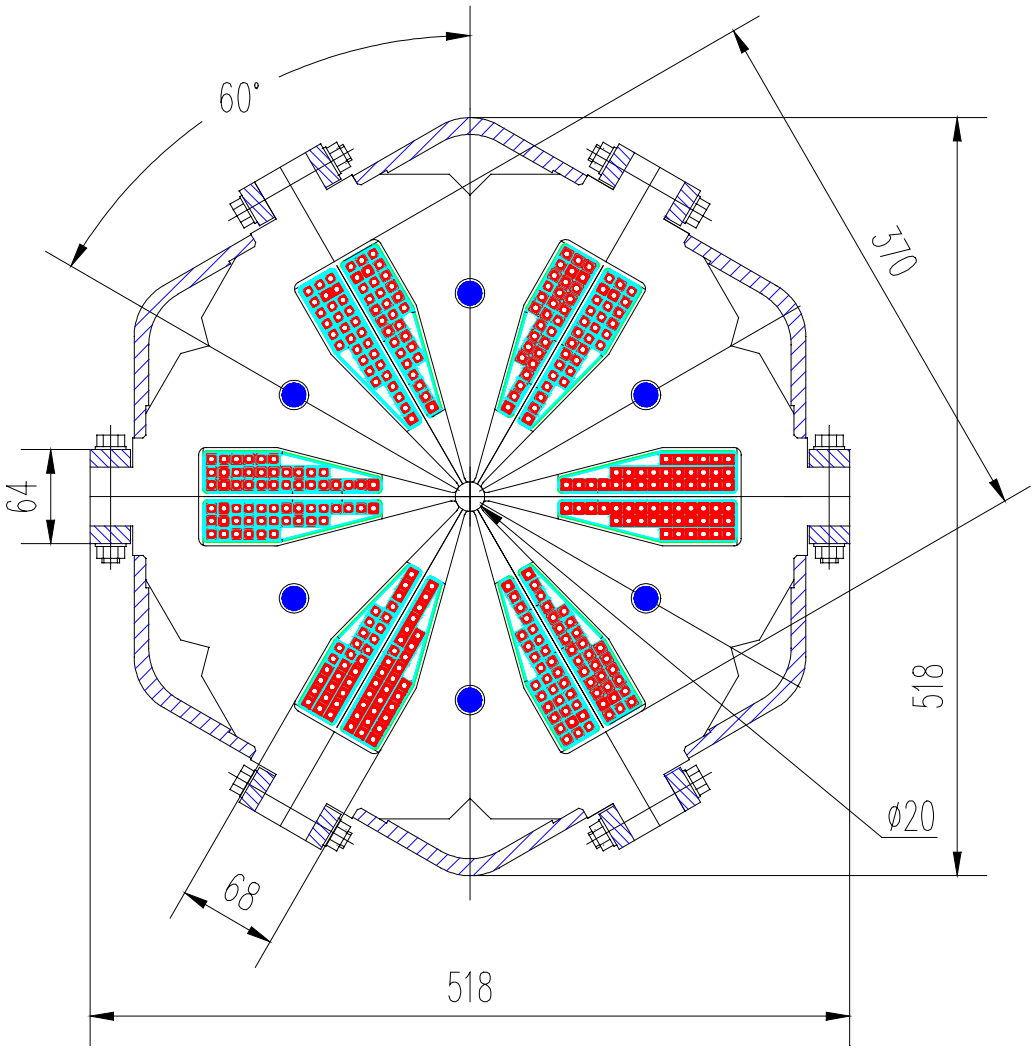

Fig. II.16. The cross section of the sextupole

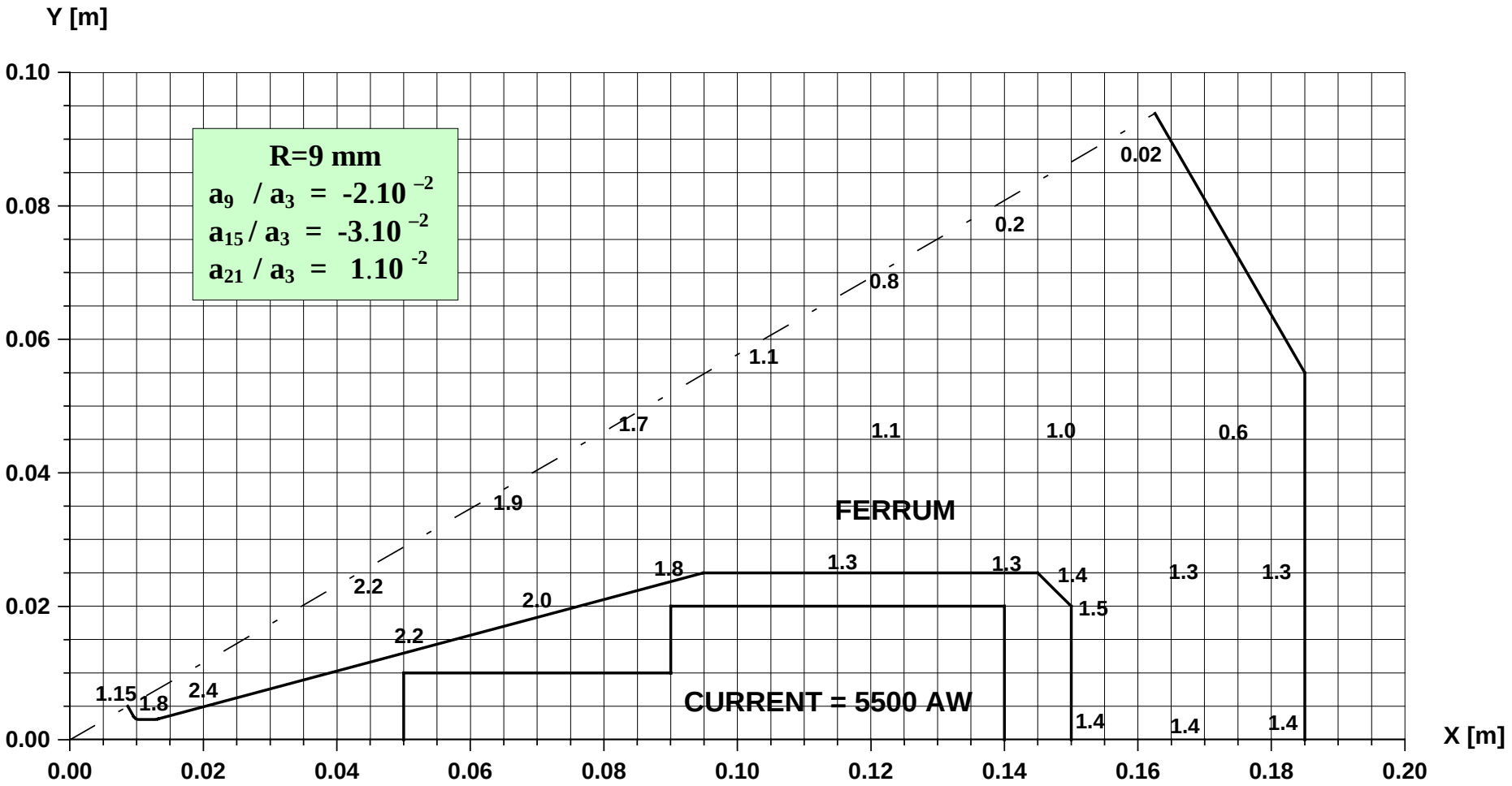

Fig. II.17 The calculated magnetic induction B[T] in some points for half pole of the sextupole

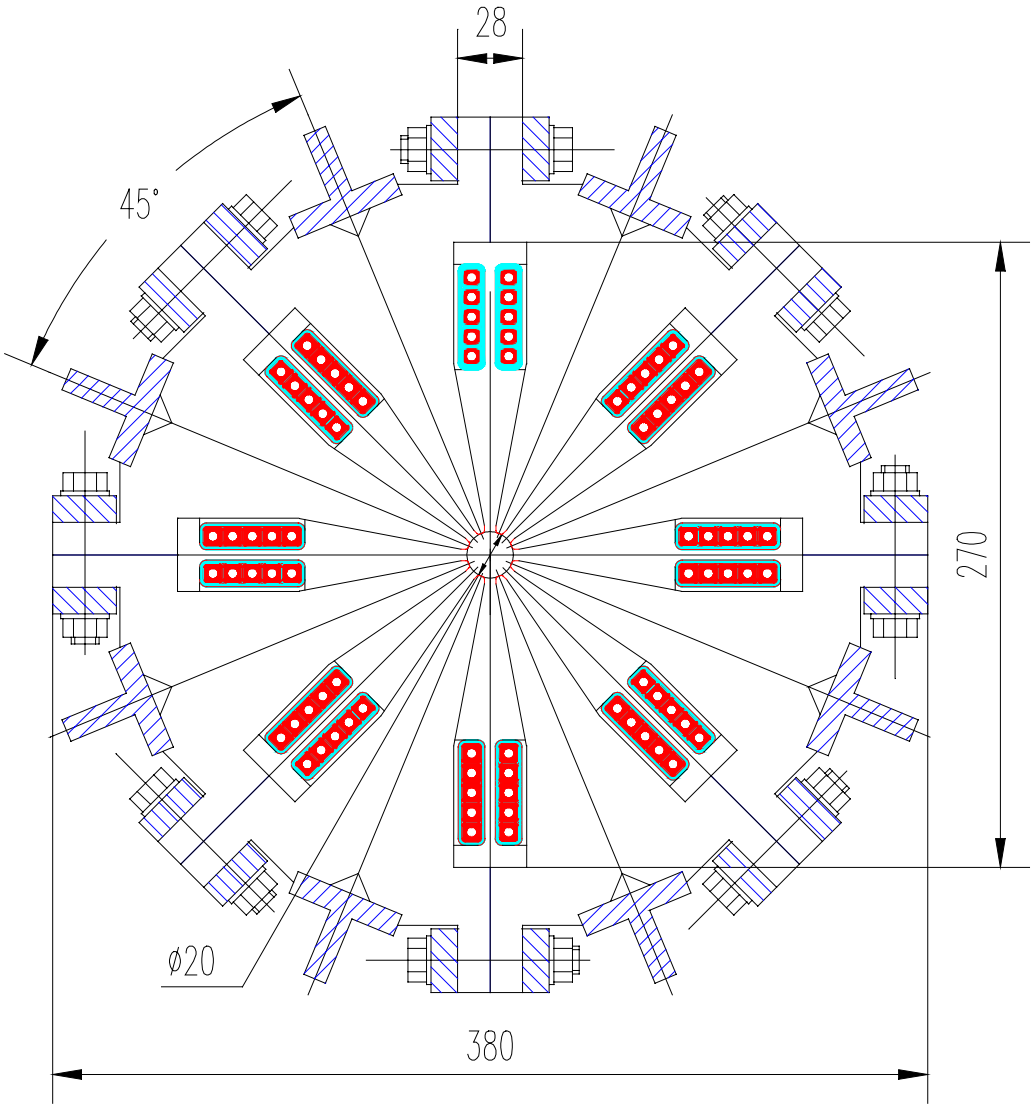

Fig. II.18. The cross section of the octupole